Journal of Power Sources 194 (2009) 730–736

Contents lists available at ScienceDirect

Journal of Power Sources

journal homepage: www.elsevier.com/locate/jpowsour

Implantation of Nafion® ionomer into polyvinyl alcohol/chitosan composites to form novel proton-conducting membranes for direct methanol fuel cells

Yuwei Zhang [a], Zhiming Cui [a], Changpeng Liu [a], Wei Xing [a,*], Jiujun Zhang [b]

[a] State Key Laboratory of Electroanalytical Chemistry, Changchun Institute of Applied Chemistry, Graduate School of the Chinese Academy of Sciences, 5625 Renmin Street, Changchun 130022, Jilin, PR China
[b] Institute for Fuel Cell Innovation, National Research Council of Canada, 4250 Wesbrook Mall, Vancouver, BC, Canada V6T 1W5

ARTICLE INFO

Article history:
Received 27 April 2009
Received in revised form 8 June 2009
Accepted 8 June 2009
Available online 17 June 2009

Keywords:
Polyvinyl alcohol
Chitosan
Nafion® ionomer
Methanol permeability
Proton conductivity
Direct methanol fuel cells

ABSTRACT

A series of cost-effective, proton-conducting composite membranes, comprising of Nafion® ionomer, chitosan (CS), and polyvinyl alcohol (PVA), is successfully prepared. By taking advantage of the strong electrostatic interactions between Nafion® ionomer and CS component, Nafion ionomer is effectively implanted into the PVA/CS composite membranes, and improves proton conductivity of the PVA/CS composite membranes. Furthermore, this effect dramatically depends on the composition ratio of PVA/CS, and the optimum conductivity is obtained at the PVA/CS ratio of 1:1. The developed composite membranes exhibit much lower methanol permeability compared with the widely used Nafion® membrane, indicating that these novel membranes have great potential for direct methanol fuel cells (DMFCs).

1. Introduction

As clean and efficient energy-conversion devices, fuel cells have been the subject of the active research for over several decades with the hope of contributing sustainable solutions to meet worldwide energy demands [1–3]. Among the various types of fuel cells, direct methanol fuel cell is considered one of the most attractive candidates in terms of its simple fabrication procedures and high-energy efficiency.

However, several challenges hinder the commercialization of direct methanol fuel cells (DMFCs), including low catalyst activity towards methanol oxidation at the anode, and high methanol crossover of the proton exchange membrane [4,5]. Particularly, methanol crossover typically results in mixed potential, catalyst poisoning as well as low fuel efficiency because of direct methanol oxidation at the cathode [6,7]. Extensive research has been carried out in the area of new membrane development, with a focus on methanol crossover reduction [8–14].

Among the membranes explored, commercially available Nafion® membranes are still the state-of-the-art and most practical membranes for DMFCs, mainly due to their high proton conductivity and high stability [15,16]. However, the level of methanol crossover for Nafion® membranes is too high at low temperatures to satisfy DMFC requirements [17]. In addition, high cost also hinders their commercial usage in DMFCs. In the effort to reduce methanol crossover, numerous approaches have been proposed, including doping organic and inorganic materials into the membranes [17–27]. Nevertheless, drawbacks of these approaches included proton conductivity scarification, mechanical stability reduction, as well as increased cost. In addition to doping with organic and inorganic materials, another way to tackle the crossover issue is to coat a thin layer of methanol barrier on the anode side of a perfluorosulfonic membrane surface [28]. Unfortunately, this surface modification also significantly decreases proton conductivity by blocking the proton transfer pathways to the main body of the membrane.

Alternatively, pore-filling membranes, comprising of a porous substrate and a filling polymer electrolyte, have also been developed so far [29,30]. These membranes have demonstrated promising performances, such as high proton conductivity and low methanol crossover. However, this strategy also faces some challenges, such as the mechanical stability of the filling. The attachment between the substrate and the filling ionomer is simply a mechanical one rather than a chemical bonding, and therefore is not sufficiently strong or stable during the electrochemical reactions. To overcome this limitation, the electrostatic interactions between the oppositely charged polyions can be used to immobilize the proton-conducting polymer onto the microstructure of the membrane

* Corresponding author. Tel.: +86 431 85262223; fax: +86 431 85685653.
E-mail address: xingwei@ciac.jl.cn (W. Xing).

0378-7753/$ – see front matter © 2009 Elsevier B.V. All rights reserved.
doi:10.1016/j.jpowsour.2009.06.022

substrate. In this way, the stability could be effectively improved. In our previous work [21], we employed this electrostatic interaction and fabricated a proton-conducting membrane based on Nafion® substrate material and chitosan (CS) coating film. This cost-effective membrane showed relatively talent immobilization of CS on Nafion membranes. However, as substrate material, chitosan membrane reveals weak mechanical strength and low proton conductivity. For a further approach, a second component, water-soluble polyvinyl alcohol (PVA), was blended into this membrane in order to enhance the mechanical property. As a result, a polyvinyl alcohol and chitosan (PVA/CS) composite membrane was obtained, possessing excellent properties such as flexibility, depressed swelling ability, and low methanol permeability. Unfortunately, the proton conductivity of such a PVA/CS composite membrane was still insufficient for DMFC applications.

To improve the conductivity of the PVA/CS membranes, in this study we used these composite membranes as the substrate and Nafion® ionomer as the filling polymer to obtain a pore-filling-like composite membrane. In this way, the PVA/CS composite membranes could mechanically block the methanol crossover, while the filling polymer (Nafion® ionomer) could provide the proton conductivity. The electrostatic interaction between the polyanion (Nafion®) and polycation (CS) could tightly immobilize Nafion® on the substrate, with deep penetration into the bulk, as shown in Scheme 1. In this study, we also varied the ratio between PVA and CS in the substrate membrane in order to determine an optimal substrate for methanol crossover reduction. The performance of the resulting Nafion® ionomer-implanted PVA/CS membranes was tested, and the results demonstrated that methanol permeability is strongly dependent on both membrane composition and morphology.

2. Experimental

2.1. Materials

Chitosan (CS) powder was purchased from Haidebei Ltd. in China. This material has a 95% degree of deacetylation and a molecular weight of 50,000 g mol^{-1}. Polyvinyl alcohol (PVA), purchased from Beijing YiLi Ltd. in China, has an average molecular weight of 80,000 g mol^{-1} and an 88% degree of alcoholysis. 5% (w/v) of Nafion® solution was purchased from Du Pont Co. All other chemicals were of analytical grade and used without further purification.

2.2. Membrane preparation

A series of PVA/CS membranes with different composition ratios was prepared by the following procedure. A 1% (w/v) CS solution was prepared by dissolving CS powder in 2% (v/v) acetic acid solution. After the CS powder was fully dissolved, the solution was then filtered and left quiescent for 2 h at ambient temperature. An aqueous solution of 5% PVA was prepared by thoroughly dissolving the PVA powder in hot water at 90 °C. When these two solutions were ready, a mixing process was performed to obtain the mixed solutions of CS and PVA in different ratios. In this step, the solution was stirred constantly for 12 h at ambient temperature, and then stored until all the entrapped gas bubbles disappeared. Afterward, the mixture solution was casted onto a flat glass substrate to form a PVA/CS composite membrane, which was dried at 80 °C for 3 h and then heated at 140 °C for 30 min. Next, this as-deposited membrane was detached from the glass substrate and washed thoroughly with deionized water prior to drying at 80 °C for 3 h, yielding a PVA/CS composite membrane. This membrane was then immersed into 5% Nafion® solution for 24 h prior to being dried at 80 °C for 3 h. Finally, it was immersed in a 1 M H_2SO_4 solution for 30 min then kept in deionized water at ambient temperature until the measurements were conducted.

2.3. Measurements for swelling properties

The swelling properties of the PVA/CS membranes were determined using water uptake measurements. The detailed procedure for water uptake and swelling property measurements was as follows. The first step was to completely dry the membrane at 80 °C for 3 h before weighing and measuring it. After that, the membrane sample was placed into deionized water at ambient temperature for 3 h to allow water uptake. The swollen membrane was then taken out of the water and quickly wiped using filter paper to remove the remaining water on both sides of the membrane; the swollen membrane was then weighed and measured. The quantity of water uptake inside the membrane was calculated according to Eq. (1):

$$\text{Water uptake}(\%) = 100\frac{W_{\text{wet}} - W_{\text{dry}}}{W_{\text{dry}}} \quad (1)$$

where W_{wet} and W_{dry} are the weights of the membrane after and before water uptake, respectively.

The changes of width of the Nafion-PVA/CS membranes in water are calculated by the following equation:

$$\Delta L(\%) = 100\frac{L_{\text{wet}} - L_{\text{dry}}}{L_{\text{dry}}} \quad (2)$$

where L_{wet} and L_{dry} are the lengths of the membrane after and before water uptake, respectively.

The methanol uptake measurement accords with the process of measuring water uptake

2.4. Instrument characterization of the membranes

2.4.1. Fourier transform infrared spectroscopy (FTIR)

The FTIR spectra were recorded in a wave number range of 4000–500 cm^{-1} with a resolution of 4 cm^{-1} using a Bruker Vertex 70 RTIR spectrometer.

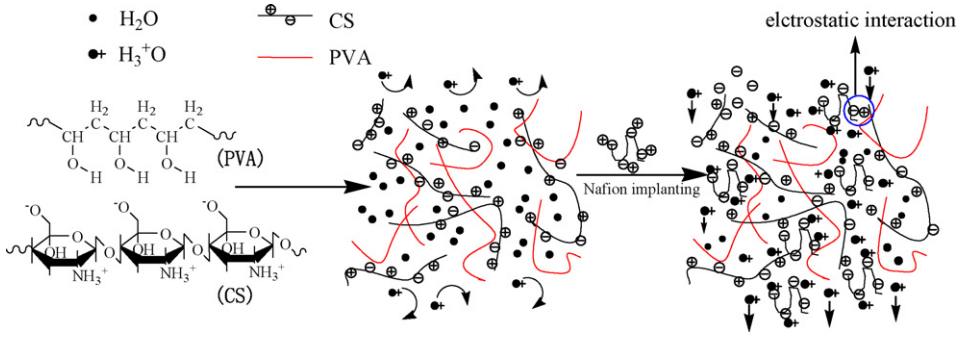

Scheme 1. Scheme for the formation of Nafion® ionomer-implanted PVA/CS composite membrane.

2.4.2. Conductivity measurements using a four-electrode cell

The proton conductivity of the membranes was measured with a four-electrode conductivity cell that had two outer gold wires for current and two inner gold wires for voltage [31]. The AC impedance spectra were measured using a Princeton Applied Research Model 273A Potentiostat (Model 5210 frequency response detector, EG&G PARC, Princeton, NJ) in the frequency range of 0.1 Hz to 100 kHz, with an AC perturbation voltage of 10 mV. For the wet membrane, conductivity measurements were carried out with the conductivity cell immersed in liquid water. The proton conductivity (σ) of the membrane was calculated using Eq. (3):

$$\sigma = \frac{L}{RA} \tag{3}$$

where L, R, and A are the distance between the two inner gold wires, the in-plane resistance of the membrane, and the cross-sectional area of the membrane, respectively.

2.4.3. Thermal analysis

A PerkinElmer 7 series thermal analysis system was used for differential scanning calorimetry (DSC) of the membranes. During the measurements, the membrane sample was heated in a N_2 flowed oven from 20–230 °C at a heating rate of 10 °C min^{-1}.

2.4.4. Atomic force microscopy (AFM)

To examine the surface morphology of the membranes, a SPI3800N atomic force microscope (AFM) (Seiko Instrument Inc.) was employed in tapping mode and with a 2 N m^{-1} probe at a scan rate of 1.44 Hz, under ambient conditions.

2.4.5. X-ray photoelectron spectroscopy (XPS)

XPS was used to detect the Nafion® ionomer distribution on the membrane surfaces. A Thermo ESCALAB 250 with monochromatized Al Kα at $h\upsilon$ = 1486.6 eV collected XPS spectra of the membrane samples. The obtained binding energies were calibrated with the C 1s peak at 284.6 eV.

2.4.6. Energy dispersive spectroscopy (EDS)

The distribution of Nafion® inside the membrane was determined using a GENESIS 2000 energy dispersive spectrometer (EDAX Inc).

2.5. Measurements of methanol permeability

The methanol permeability of the membranes was determined and calculated by the method described in our previous paper [31]. The methanol concentration in the receptor chamber was measured versus time using a gas chromatograph (Shimadzu GC-14B) equipped with a thermal conductivity detector.

3. Results and discussion

3.1. Membrane water uptake and swelling

The swelling property has a profound effect on proton transport and dimensional stability of proton-conducting membranes. Proton transport requires a significant amount of water to coordinate with protons. However, excessively high levels of water uptake can result

Table 1
Water uptake and swelling coefficients of the composite membranes.

Mixing ratio of PVA and CS	2:1 (%)	3:2 (%)	1:1 (%)	1:2 (%)	1:4 (%)
Water uptake (PVA/CS)	159	110	81	73	67
Water uptake (Nafion-PVA/CS)	92	65	45	41	95
Swelling coefficient (PVA/CS)	27	25	20	41	43

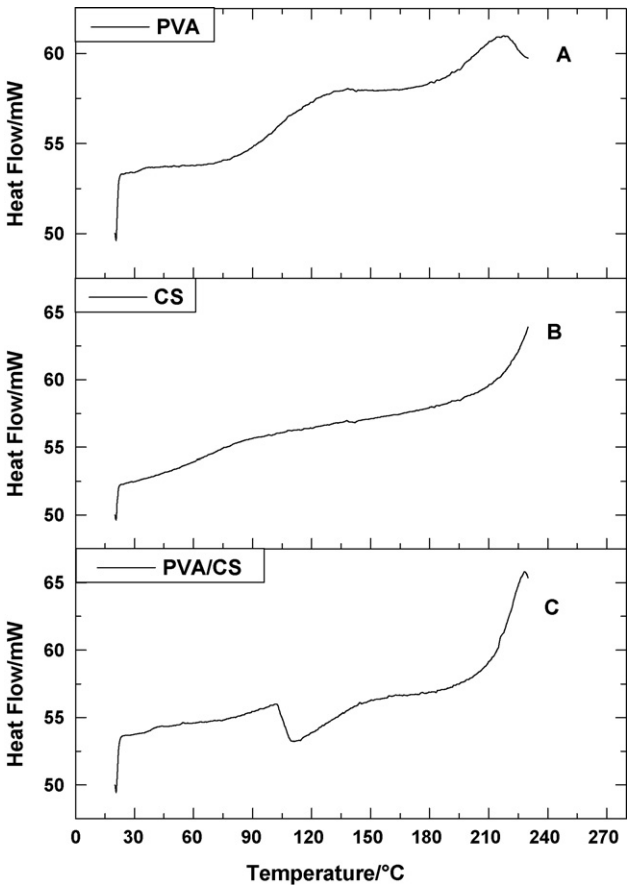

Fig. 1. Differential scanning calorimetry curves: (A) pure PVA; (B) pure CS; and (C) PVA/CS composite membranes.

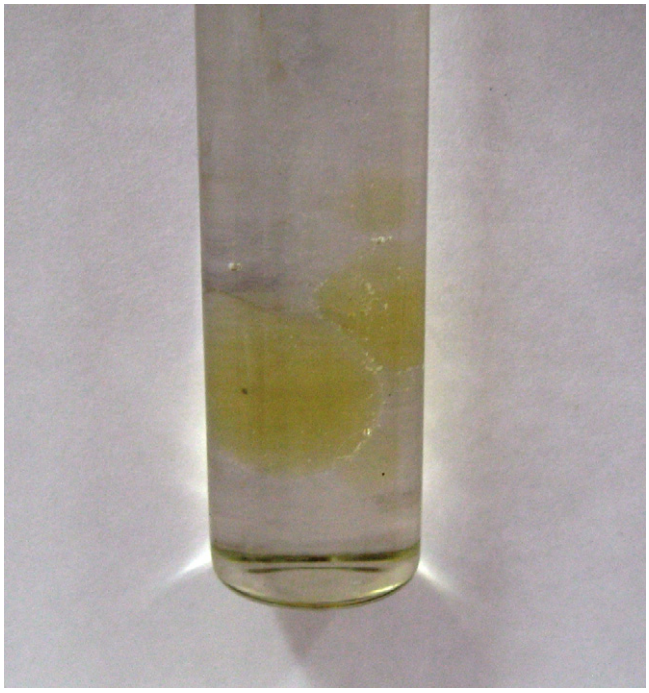

Scheme 2. The insoluble complex formed by dropping chitosan solution into Nafion® solution.

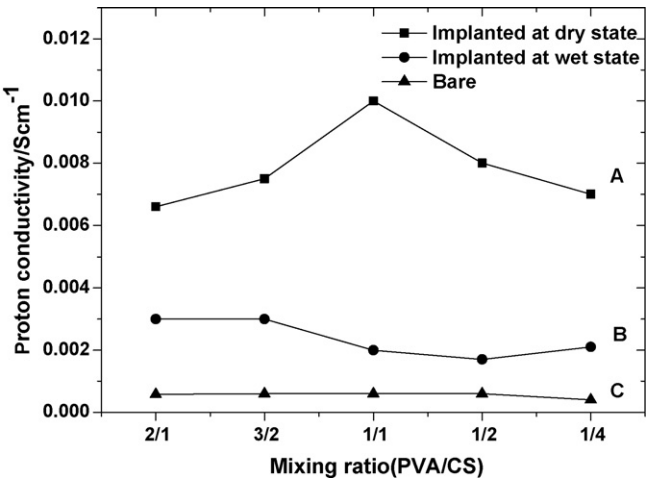

Fig. 2. Proton conductivities of PVA/CS composite membranes at ambient temperature: (A) implanted at dry state with Nafion® ionomer; (B) implanted at wet state with Nafion® ionomer; and (C) bare composite membrane.

in the dimensional change of membranes, which leads to the loss of mechanical properties. Table 1 shows the water uptake and swelling properties of the composite membranes. It seems that membrane swelling always happens, regardless of the ratio of PVA to CS in the membranes. However, it can be seen from Table 1 that the 1:1 ratio of PVA to CS, with a swelling coefficient of 20% and a water uptake of 81%, is the best among these membranes.

3.2. Thermal analysis

The interaction of polyvinyl alcohol and chitosan in the composite membrane can significantly affect the membrane properties. For comparison, the DSC curves obtained for pure PVA, pure CS, and PVA/CS composite are shown separately in Fig. 1. For pure PVA and pure CS, the glass transition temperatures are around 103 °C and 68 °C, as shown in Fig. 1A and B, respectively. For PVA/CS composite membrane, an exothermic peak appears at 100 °C, as shown in Fig. 1C. This new peak may indicate the formation of a new crystal phase, suggesting that the composite membrane may not be a simple mixture of PVA and CS. A much higher melting point of 213 °C is associated with the formation of this new phase. It is indicated that the formation of this new phase inside the composite membrane may be responsible for the improved thermal stability as compared with membranes of pure CS or pure PVA.

3.3. Proton conductivity

The proton conductivity of membranes is one of the most crucial parameters for evaluating a proton exchange membrane. In our studies, the proton conductivities for pure PVA and PVA/CS composite membranes were found to be 2.45×10^{-3} S cm^{-1} and 6×10^{-4} S cm^{-1}, respectively. These values are too low for practical use in DMFCs. After the implantation of Nafion® ionomer inside these membranes, the proton conductivity becomes much higher. For example, a Nafion® ionomer-implanted PVA/CS membrane could give a proton conductivity of 0.01 S cm^{-1} at ambient temperature, which is nearly 17 times higher than that of as-deposited PVA/CS membrane. This significant increase in proton conductivity suggests that some Nafion® ionomer chains had been implanted into the bulk PVA/CS membrane. This strong attachment of Nafion® polymer into the pores of the PVA/CS composite membrane is due to the electrostatic interactions between Nafion® ionomer and CS components [21], as shown in Scheme 2.

Experiments also showed that the Nafion® ionomer immobilization inside the composite membrane could be strongly affected by the dry and wet membrane states. For example, as shown in

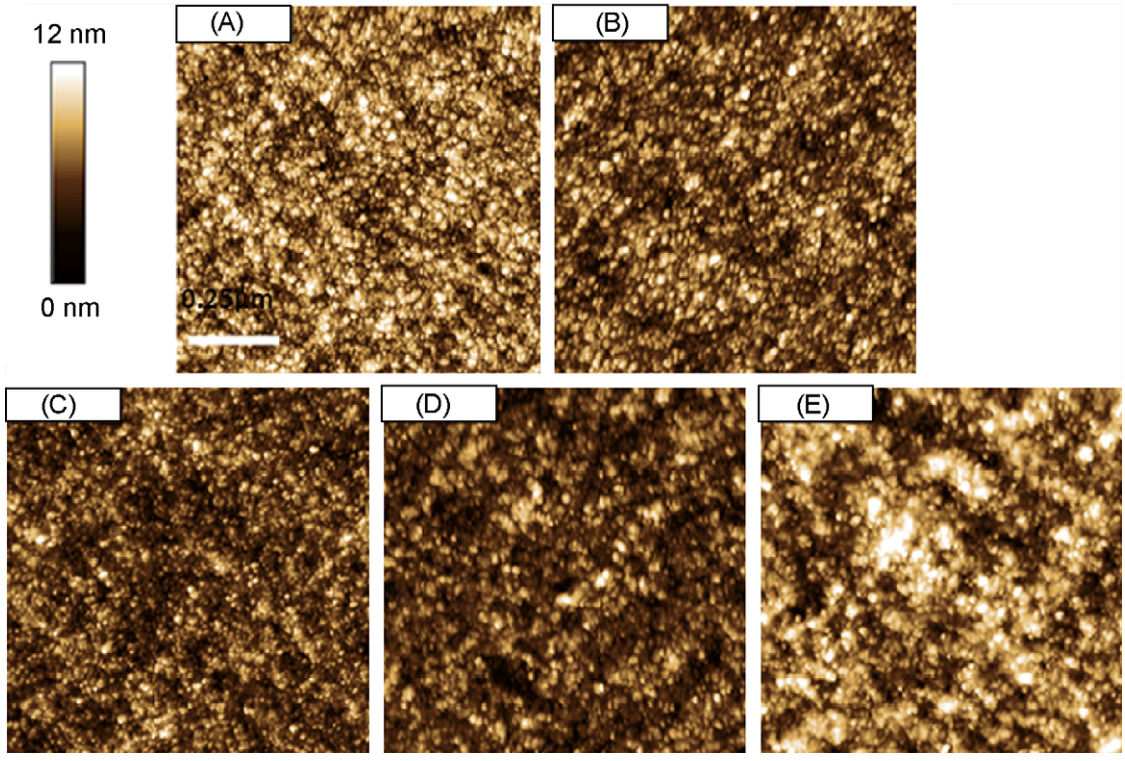

Fig. 3. AFM pictures of the composite membranes: (A) PVA/CS ratio of 2:1; (B) PVA/CS ratio of 1.5:1; (C) PVA/CS ratio of 1:1; (D) PVA/CS ratio of 0.5:1; (E) PVA/CS ratio of 0.25:1.

Fig. 2, if the Nafion® ionomer was immobilized in a dry PVA/CS composite membrane, the resulting proton conductivity could be much higher than when the Nafion® ionomer was immobilized in a wet membrane. This could be attributed to the different thermodynamic driving forces for Nafion® implantation into the bulk of the membrane. The driving force for Nafion® implantation through electrostatic interaction inside the composite membrane at dry state is much higher than that at wet state. The stronger driving force for solvent/Nafion® ionomer chains in a dry membrane could make more Nafion® ionomer chains enter the inner regions of the dry membrane along with the solvent.

The ratio of PVA to CS in the composite membrane could also affect the proton conductivity. As shown in Fig. 2A, the proton conductivity increases monotonically with increasing CS content up to a ratio of 1:1, and then declines when the ratio is further increased. This phenomenon indicates that the composition ratio plays a role in controlling the microstructure or network of PVA/CS composite membranes, which then affects the Nafion® ionomer distribution inside the membrane.

In order to further study the PVA/CS composition ratio dependency of proton conductivity, as observed in Fig. 2, atomic force microscopy was employed to evaluate the morphology of dry PVA/CS membranes with different compositions. The obtained results are shown in Fig. 3. In these pictures, the lighter spots correspond to the PVA-rich areas, while the darker spots are CS-rich areas. It can be seen from these images that the degree of uniformity of the PVA and CS distributions varies with the different ratios. Among these different ratios, 1:1 PVA/CS gives the best homogeneous distribution of PVA and CS. Although the inner structure of the membrane cannot be directly detected from these images, they must reflect the inner microstructures to some extent. It is indicated that the best homogeneous distribution of PVA and CS in the composite should give the best distribution of implanted Nafion® ionomer, resulting in the highest proton conductivity, as observed in Fig. 2.

3.4. Active energy for proton transport across the composite membrane

The temperature dependency of membrane proton conductivity was also measured in this study to obtain the active energies of proton transport, as shown in Fig. 4. The Arrhenius plots in Fig. 4 all show linear tendencies, suggesting that the protons transfer predominantly via a vehicle mechanism in the composite membranes. The relationship between the proton conductivity (σ) and the reciprocal of temperature can be expressed as an Arrhenius plot (Eq. (4)):

$$\ln\sigma = \ln\sigma^{\circ} - \frac{E_a}{RT} \quad (4)$$

Where σ° is the proton conductivity at unlimited temperature, E_a is the active energy of proton transport, R is the universal gas constant, and T is the temperature in Kelvin. According to Eq. (4), the activation energies for the composite membranes with PVA/CS ratios of 2:1, 1.5:1, 1:1, 0.5:1, and 0.25:1 were calculated to be 8.3, 8.8, 13.7, 11.4, and 9.2 kJ mol^{-1}, respectively. The high values for ratios 1:1 and 0.5:1 membranes may suggest a different mechanism for proton transport in these two membranes. In the literature [32], a Grotthuss mechanism for proton transport was proposed with active energies of 14–40 kJ mol^{-1}. The values for these two membranes are close to this range, suggesting that the corresponding proton transport may follow a Grotthuss mechanism. For ratios of 2:1, 1.5:1, and 0.25:1, the low activation energies may be attributed to the free hydroxyl and amino groups present in the polyelectrolyte, which could give rise to some hydrophilic regions in the membrane, thereby affecting proton transport [32].

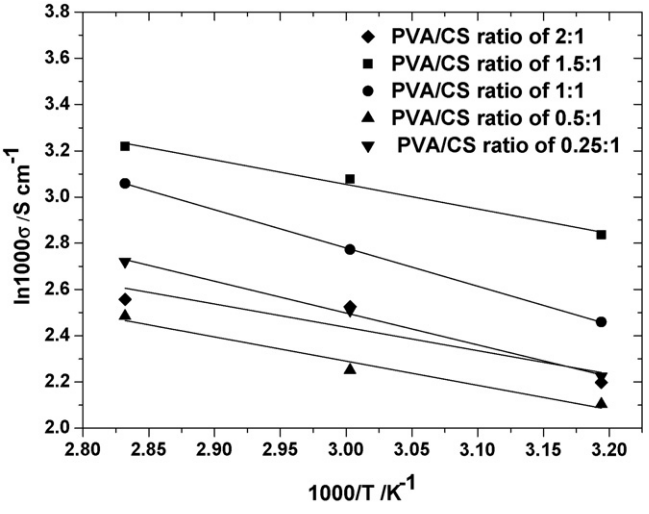

Fig. 4. Arrhenius plots (ln(1000σ) vs. 1000/T) of proton conductivity (σ) as a function of temperature for PVA/CS composite membranes.

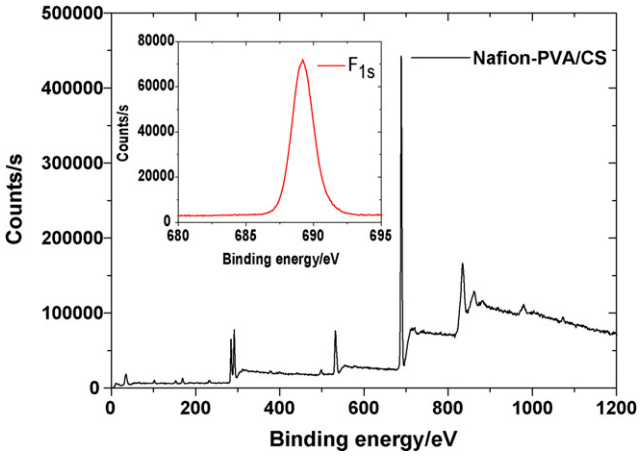

Fig. 5. XPS spectrum of Nafion®-PVA/CS composite membrane with a PVA/CS ratio of 1:1. The inset spectrum shows the peak of F_{1S}.

3.5. Nafion® distribution inside the membrane

The membrane surface and inner distributions of Nafion® ionomer were also investigated using both XPS and EDS methods. The fluorine element (F_{1s}) was used as an indicator for Nafion® content. In general, the average detecting depths using XPS and EDS under normal conditions are ca. 5–10 nm and 4–6 μm, respectively. Fig. 5 shows the XPS spectrum of a composite membrane with a PVA/CS ratio of 1:1. With the obtained F_{1s} peaks, the surface content of fluorine was calculated to be 33.2 atom ratio% (At.%). Fig. 6 shows the EDS spectra of the same membrane sample as in Fig. 5. From Fig. 6, the average fluorine content inside the thicker layer was calculated to be 12.9 At.%. Note that the 33.2 At.% or 12.9 At.% represents the number of atoms out of the total atoms of the surface layer (~5 nm) or inner layer (~5 μm) of the membrane. Here we define these two values as $C_{surface}$ and C_{inner}, respectively. While we assume that the bulk concentration of Nafion® ionomer across the membrane may be uniformly distributed, the relative bulk concentration (C_{bulk}) of Nafion® ionomer inside the membrane should be obtainable based on these $C_{surface}$ and C_{inner} values as well as the equations described below. The numbers of fluorine atoms inside the surface and the thick layers can be expressed as $F_{surface}$ and

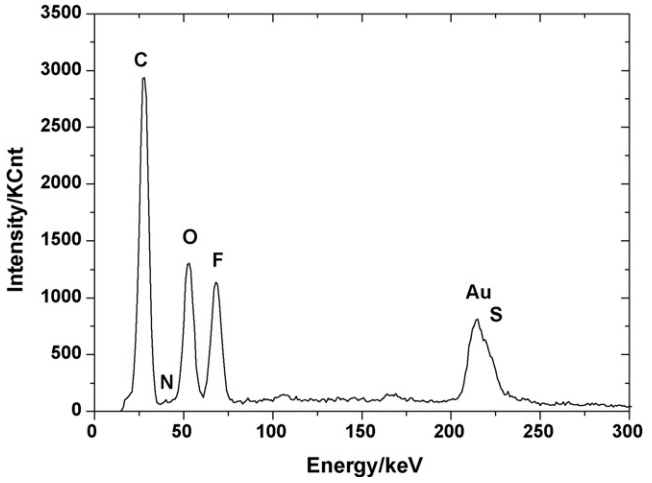

Fig. 6. Energy dispersive spectrum of Nafion®-PVA/CS composite membrane with a PVA/CS ratio of 1:1.

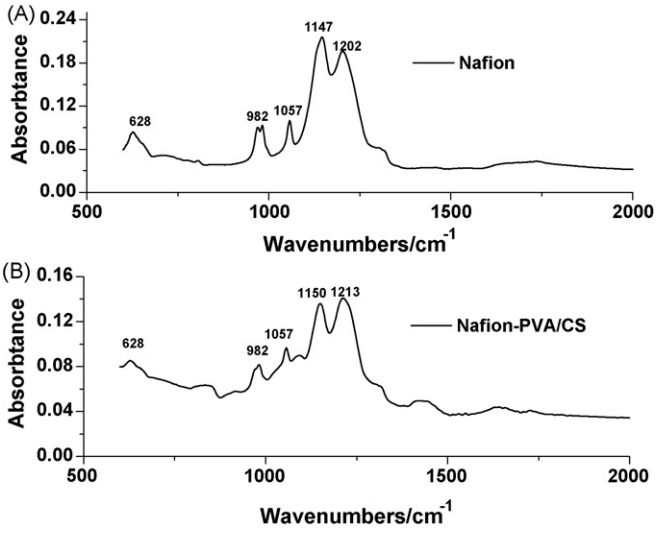

Fig. 7. FTIR spectra of (A) Nafion® ionomer and (B) Nafion® ionomer-implanted PVA/CS composite membrane.

F_{inner}, respectively. The numbers of total atoms inside the surface and the thick layers can be expressed as $N_{surface}$ and N_{inner}, respectively. Then $F_{surface}$ and F_{inner} can be related to $C_{surface}$ and C_{inner} by the following equations:

$$F_{surface} = N_{surface}C_{surface} \quad (5)$$

$$F_{inner} = N_{inner}C_{inner} \quad (6)$$

Because the test depth of EDS is 1000 times of that of XPS, the relationship between N_{inner} and $N_{surface}$ can be expressed as Eq. (7):

$$N_{inner} = 1000N_{surface} \quad (7)$$

Combining Eqs. (5), (6), and (7), the following relationship can be obtained:

$$\frac{1000C_{inner}}{C_{surface}} = \frac{F_{inner}}{F_{surface}} \quad (8)$$

Using the values of 33.2 At.% and 12.9 At.% as $C_{surface}$ and C_{inner} obtained from the XPS and EDS measurements, the following relationship can be deduced from Eq. (8):

$$F_{inner} = 389F_{surface} \quad (9)$$

For the relative bulk concentration of Nafion® ionomer inside the membrane, the following equation can be used:

$$C_{bulk} = \frac{F_{inner} - F_{surface}}{N_{inner} - N_{surface}} \quad (10)$$

The calculated C_{bulk} value based on Eq. (10) was 12.9 At.%. This value was the same as that of C_{inner} measured by EDS. Because the surface layer (~5 nm) measured by XPS is much thinner than the inner layer (~5 μm) measured by EDS, the value of $F_{surface}$ or $N_{surface}$ is negligibly smaller than F_{inner} or N_{inner} in Eq. (10). Therefore, Eq. (10) could be approximately simplified as Eq. (11):

$$C_{bulk} = \frac{F_{inner}}{N_{inner}} \quad (11)$$

Eq. (11) suggests that the concentration distribution in the inner layer as measured by EDS may represent the bulk concentration of Nafion® ionomer inside the composite membrane.

3.6. Interaction between the negatively charged group ($-SO_3^-$) of the Nafion® ionomer and the positively charged group ($-NH_3^+$) in the CS group

In order to probe the possible interaction between the negatively charged group ($-SO_3^-$) of the Nafion® ionomer and the positively charged group ($-NH_3^+$) in the CS group inside the composite membrane, the FTIR spectra of Nafion® ionomer and Nafion® ionomer-implanted PVA/CS composite membrane were recorded, as shown in Fig. 7A and B. In the spectrum for Nafion® ionomer (Fig. 7A), four major vibrational fingerprint peaks can be found. The peak at 1202 cm^{-1} is for the CF_2 and SO_3^- groups, the peak at 1147 cm^{-1} for the CF_2 group, the peak at 1057 cm^{-1} for the SO_3^- group, the peak at 982 cm^{-1} for the C–O–C group, and the peak at 626 cm^{-1} for CF_2 [33]. After the implantation (Fig. 7B), these five peaks can still be observed, suggesting that the Nafion® ionomer structure is still maintained in the implantation process. However, the major peaks for the–SO_3^- group at 1147 cm^{-1} and 1202 cm^{-1} are shifted to higher positions of 1150 cm^{-1} and 1213 cm^{-1}, respectively. These shifts may indicate the interaction between the negatively charged group ($-SO_3^-$) of Nafion® ionomer and the positively charged group ($-NH_3^+$) in the CS group.

3.7. Methanol crossover

Methanol crossover, which occurs due to diffusion as a result of the concentration gradient and also the electro-osmotic drag, is a critical problem for DMFC membranes. Decreasing methanol diffusion and correction of electro-osmotic drag effects were developed and found necessary for protonic membranes [34,35]. In order to verify the feasibility of using these Nafion® ionomer-implanted PVA/CS composite membranes for direct methanol fuel cells, the methanol permeability was measured for membranes with different PVA/CS ratios. The obtained results are shown in Fig. 8. It can be seen that the lowest methanol permeability was obtained using a membrane with a PVA/CS ratio of 1:1. Compared to a Nafion® membrane, which has a methanol permeability of 4.6×10^{-6} cm^2 s^{-1}, the Nafion® ionomer-implanted PVA/CS composite membranes have lower values, in the range of 1.0×10^{-6}–2.2×10^{-6} cm^2 s^{-1}. We have also determined the methanol uptake, the results show that the methanol uptake of Nafion-PVA/CS (approximately 1%) is trivial compared to Nafion (63.77%). It indicates that the methanol crossover of Nafion-PVA/CS caused by elecro-osmosis is much more lower than that of Nafion. Therefore, the membranes developed in this study have advantages in terms of methanol crossover and cost reduction, indicating that they should be good candidates for DMFC applications. Further work has been scheduled to validate these membranes in a DMFC environment.

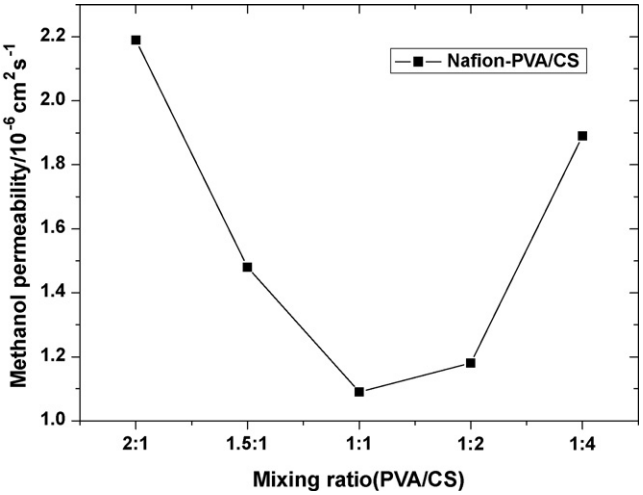

Fig. 8. Methanol permeability of Nafion® ionomer-implanted PVA/CS composite membrane at ambient temperature.

4. Conclusions

In the effort to reduce methanol crossover and the cost of DMFC membranes, a series of cost-effective proton-conducting composite membranes comprised of Nafion® ionomer, CS, and PVA were successfully prepared. Results showed that the implantation of Nafion® ionomer into the PVA/CS composite membrane effectively improves the proton conductivity. This implantation is attributed to the strong electrostatic attractions between Nafion® ionomer and CS detected by FTIR measurements. This interaction facilitates deep penetration of the conductive ionomer into the bulk of the composite, as well as strong immobilization on the substrate. The concentration of the implanted Nafion® ionomer inside the membrane was also measured using EDS, yielding a value of 12.9 At%. The composition ratio between PVA and CS can also affect the proton conductivity. Optimal conductivity was obtained with a 1:1 ratio of PVA/CS. At this ratio, atomic force microscopy detected the best homogeneous mixing of PVA and CS, which facilitates a better distribution of Nafion® ionomer in the composite membrane and generates higher proton conductivity. The developed composite membranes were also tested for methanol permeability. These membranes exhibit much lower methanol permeability when compared with the widely used Nafion® membrane, suggesting that the composite membranes are good candidates for DMFC applications in terms of both methanol crossover reduction and low cost.

Acknowledgements

This work is supported by the Chinese High Technology Research Program (863 Program, 2007AA05Z159) and the Chinese Nature Science Foundation (20433060). Professor Wei Xing also wishes to thank the Institute for Fuel Cell Innovation, National Research Council of Canada (NRC-IFCI) for its support during his time as a visiting researcher.

References

[1] R.G. Rajendran, MRS Bulletin 30 (2005) 587–590.
[2] B. Smitha, S. Sridhar, A.A. Khan, Journal of Membrane Science 259 (2005) 10–26.
[3] G. Wegner, Polymers as functional components in batteries and fuel cells, in: 8th International Symposium on Polymers for Advanced Technologies, John Wiley & Sons Ltd, Budapest, HUNGARY, 2005, pp. 705–708.
[4] S. Wasmus, A. Kuver, Journal of Electroanalytical Chemistry 461 (1999) 14–31.
[5] H.S. Liu, C.J. Song, L. Zhang, J.J. Zhang, H.J. Wang, D.P. Wilkinson, Journal of Power Sources 155 (2006) 95–110.
[6] J. Cruickshank, K. Scott, Journal of Power Sources 70 (1998) 40–47.
[7] M.K. Ravikumar, A.K. Shukla, Journal of the Electrochemical Society 143 (1996) 2601–2606.
[8] J. Saito, K. Miyatake, M. Watanabe, Macromolecules 41 (2008) 2415–2420.
[9] D. Yamamoto, H. Munakata, K. Kanamura, Journal of the Electrochemical Society 155 (2008) B303–B308.
[10] Y.S. Choi, T.K. Kim, E.A. Kim, S.H. Joo, C. Pak, Y.H. Lee, H. Chang, D. Seung, Advanced Materials 20 (2008) 2341–2344.
[11] H.W. Zhang, X.H. Fan, J. Zhang, Z.T. Zhou, Solid State Ionics 179 (2008) 1409–1412.
[12] S.N. Xue, G.P. Yin, Polymer 47 (2006) 5044–5049.
[13] P.X. Xing, G.P. Robertson, M.D. Guiver, S.D. Mikhailenko, K.P. Wang, S. Kaliaguine, Journal of Membrane Science 229 (2004) 95–106.
[14] S. Reichman, L. Burstein, E. Peled, Journal of Power Sources 179 (2008) 520–531.
[15] H. Bunazawa, Y. Yamazaki, Journal of Power Sources 182 (2008) 48–51.
[16] H. Rivera, J.S. Lawton, D.E. Budil, E.S. Smotkin, Journal of Physical Chemistry B 112 (2008) 8542–8548.
[17] Z. Cui, Y. Xiang, T. Zhang, Acta Chimica Sinica 65 (2007) 1902–1906.
[18] T. Sancho, J. Lemus, M. Urbiztondo, J. Soler, M.P. Pina, Microporous and Mesoporous Materials 115 (2008) 206–213.
[19] Y. Zhai, H. Zhang, Y. Zhang, D. Xing, Journal of Power Sources 169 (2007) 259–264.
[20] M.A. Navarra, C. Abbati, B. Scrosati, Journal of Power Sources 183 (2008) 109–113.
[21] Z.M. Cui, N.W. Li, X.C. Zhou, C.P. Liu, J.H. Liao, S.B. Zhang, W. Xing, Journal of Power Sources 173 (2007) 162–165.
[22] M.B. Satterfield, P.W. Majsztrik, H. Ota, J.B. Benziger, A.B. Bocarsly, Journal of Polymer Science Part B-Polymer Physics 44 (2006) 2327–2345.
[23] M.A. Navarra, F. Croce, B. Scrosati, Journal of Materials Chemistry 17 (2007) 3210–3215.
[24] H. Tang, Z. Wan, M. Pan, S.P. Jiang, Electrochemistry Communications 9 (2007) 2003–2008.
[25] F.M. Vichi, M.T. Colomer, M.A. Anderson, Electrochemical and Solid State Letters 2 (1999) 313–316.
[26] J. Liu, H.T. Wang, S.A. Cheng, K.Y. Chan, Chemical Communications (2004) 728–729.
[27] F. Xu, C. Innocent, B. Bonnet, D.J. Jones, J. Roziere, Fuel Cells 5 (2005) 398–405.
[28] Z.G. Shao, X. Wang, I.M. Hsing, Journal of Membrane Science 210 (2002) 147–153.
[29] T. Yamaguchi, H. Zhou, S. Nakazawa, N. Hara, Advanced Materials 19 (2007) 592–596.
[30] T. Yamaguchi, F. Miyata, S. Nakao, Advanced Materials 15 (2003) 1198–1201.
[31] Z.M. Cui, C.P. Liu, T.H. Lu, W. Xing, Journal of Power Sources 167 (2007) 94–99.
[32] B. Smitha, S. Sridhar, A.A. Khan, Macromolecules 37 (2004) 2233–2239.
[33] A. Gruger, A. Regis, T. Schmatko, P. Colomban, Vibrational Spectroscopy 26 (2001) 215–225.
[34] X.M. Ren, T.E. Springer, T.A. Zawodzinski, S. Gottesfeld, Journal of The Electrochemical Society 147 (2000) 466.
[35] Z.Y. Jiang, X.H. Zheng, H. Wu, F.S. Pan, Journal of Power Sources 185 (2008) 85.